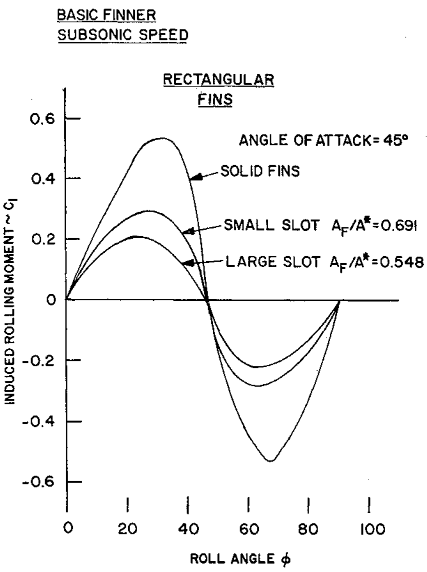

Fig. 7 Typical effect of slot on induced rolling moment.

During the Naval Academy tests, both rectangular and trapezoidal fins were studied. The results obtained were essentially the same for both types of fins.

Single-degree-of-freedom, free oscillation tests were then conducted at the Naval Academy to determine the effect on the missile's longitudinal stability due to slot size.[8] Pitching motion was recorded and these data were fit using a nonlinear, least squares technique. Both the linear and nonlinear contributions of the restoring moment and pitch damping moment were determined. The results of this study indicated that the slot reduces longitudinal stability at low angles of attack but increases it at high angles of attack. Only with extreme slot size ($AF/A^* \leq 0.347$) was the model statically unstable. No dynamic instability was present.

Returning to Fig. 4, one might conclude that the slot itself, without the presence of fin cant, actually promotes lock-in. Returning to Fig. 5, we note that this is not the case at the moderate angles of attack because the minimum lock-in angle is greater.

In order to determine if the slot promoted lock-in at higher angles of attack, a test was conducted at NSRDC to study the effect of slot size on the induced rolling moment. The basic finner[7] (a well-known research configuration) was used as the test specimen because of its availability. Fins identical to those tested at the Naval Academy were studied.

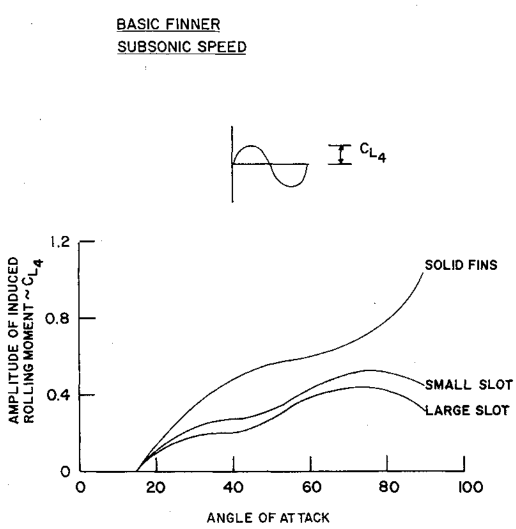

Fig. 8 Effect of slot on amplitude of induced rolling moment.

An internal strain gage balance was used to measure the induced rolling moment. The two planforms for the slot sizes shown are presented in Fig. 1. At an angle of attack of 45° (Fig. 7), the slot significantly reduces the induced rolling moment. The effect of slot size on the induced rolling moment at higher angles of attack is equally dramatic. Figure 8 summarizes the results of the test. It is noted that the induced rolling moment was reduced by as much as 70 percent for the slot sizes tested and the small slot is nearly as efficient as the large slot in reducing the induced rolling moment.

Conclusion

Based on the results of this study it is concluded that, at subsonic speeds, the slotted fin is superior to the solid fin in that it eliminates roll speed-up, appreciably reduced the induced rolling moment, and increases longitudinal stability at high angles of attack. Stability is reduced at low angles of attack. However, the possibility of catastrophic yaw is minimized.

References

[1] Nicolaids, J. D., "Missile Flight and Astrodynamics," TN 100-A, 1959–1961, Bureau of Naval Weapons, Washington, D. C.

[2] Schneller, E., "Vibrations of a Missile about Its Center of Gravity," Repts. 11, 12, and 14, Nov. 16, 1940 to June 17, 1941. Translation Foreign Document Evaluation Branch, Naval Ordnance Research and Development Center, Aberdeen Proving Ground, Md.

[3] Wingo, C. H., Jr. and Jones, F. L., "Free Flight and Catapult Tests of 250-lb. Low Drag GP Bomb, Type EX-2 MOD 2, EX-2A, 250-lb. Low Fragmentation Bomb, Type EX-17, MOD 6, 2000-lb. Low Drag GP Bomb, Type EX-11, MOD 1 with Canted Fins," Rept. 1419, Oct 1955, Naval Proving Ground, Dahlgren, Va.

[4] Lugt, H. J. "Self-Sustained Spinning of a Cruciform Fin System," *Proceedings of the Fifth United States Navy Symposium on Aeroballistics*, Naval Ordnance Lab, White Oak, Md., 1961.

[5] Daniels, P., "Fin Slots vs Roll Lock-In and Roll Speed-Up," *Journal of Spacecraft and Rockets*, Vol. 4, No. 3, March 1967, pp. 410–412.

[6] Daniels, P., "Effect of Fin Slots and Fin Tabs on the Dynamic Stability Characteristics of the Navy Low Drag Bomb," *Journal of Spacecraft and Rockets*, Vol. 7, No. 9, Sept 1970, pp. 1151–1152.

[7] Daniels, P., "A Study of the Nonlinear Rolling Motion of a Four Finned Missile," *Journal of Spacecraft and Rockets*, Vol.7, No. 4, April 1970, pp. 510–512.

[8] Clare, T. A. and Daniels, P., "Effect of Fin Slots on the Static and Dynamic Stability Characteristics of Finned Bodies," NWL TR-2582, June 1971, Naval Weapons Lab., Dahlgren, Va.

V-Wings and Diamond Ring-Wings of Minimum Induced Drag

JOHN S. LETCHER JR.*

Colorado State University, Fort Collins, Colo.

THE problems solved here should be found in the literature of the classical era of aerodynamics, and it is hard to believe that they could have been overlooked for so many decades; but it appears that the solutions have never been published. The solutions do contribute to some modern interest in nonplanar wings;[1] also the added-mass coefficients

Received February 25, 1972; revision received April 17, 1972. The author thanks H. J. Stewart, P. B. S. Lissaman, and J. Siekmann for helpful comments during preparation of this note.

Index categories: Airplane and Component Aerodynamics; Hydrodynamics.

* Assistant Professor of Mechanical Engineering, Presently Naval Architect and Engineer, Henry R. Hinckley and Co., Southwest Harbor, Maine.

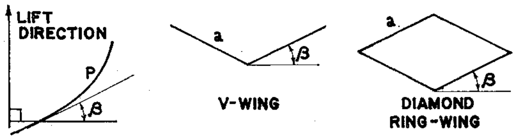

Fig. 1 Local inclination of lifting elements.

found provide new solutions for slender wings of V and diamond cross section.

The optimal induction theorem for non-planar wings was given by Munk[2]: for an airfoil system of given vertical lift and given outline P (projected onto a plane normal to the free stream), the minimum induced drag is obtained when the normal component of induced velocity is proportional to $\cos\beta$, β being the local inclination of the lifting element (Fig. 1). (For the V- and diamond-wings β is constant over the entire wing, so minimum drag corresponds to uniform normal velocity.) For this minimum drag case the vortex wake extends downstream with no change in cross-sectional shape, and a small asymptotic inclination $2w/U$ where w is the uniform downwash at the wing and U is the freestream velocity. In steady flight the lift and induced drag of the wing are exactly equivalent to the downward momentum and the energy, respectively, of the two-dimensional "Trefftz plane" flow about the moving vortex wake; in particular

$$L = MU \cdot 2w, \qquad D_i = \tfrac{1}{2}M(2w)^2 \tag{1}$$

where M is the added mass per unit length of the two-dimensional shape P defined by projection of the wing onto the Trefftz plane. The downwash w can be eliminated to give the induced-drag coefficient as

$$C_{D_i} = \tfrac{1}{4}(\rho S/M)C_L{}^2 \tag{2}$$

where ρ is the freestream density and S is the wing area, to which the force coefficients are referred.

The added mass M is a property of the cross section shape P, and is proportional to ρ and to the square of the linear dimension (such as wing span). The complex variable $z = x + iy$ is introduced in the Trefftz plane such that the origin moves downward with the same velocity $2w$ as does P (Fig. 2). Thus P is stationary in the z-plane, with zero normal velocity, while far away from the body there is a uniform flow with velocity $(2w, 0)$. If the complex velocity potential satisfying these boundary conditions, and having zero circulation about the body, is expressed in the form (A_n real)

$$f(z) = 2wg(z) = 2w\left\{z + \sum_{n=1}^{\infty} A_n z^{-n}\right\} \tag{3}$$

then Lamb[3] has shown that M can be identified with the coefficient A_1:

$$M = 2\pi\rho A_1 \tag{4}$$

This includes the mass of fluid within any closed portions of the outline. If the added mass due to the exterior flow only is required (as in slender-body theory) this is

$$M' = \rho(2\pi A_1 - Q) \tag{5}$$

where Q is the area of all closed portions.

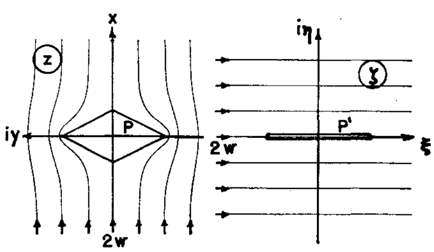

Fig. 2 Conformal mapping of Trefftz-plane flow.

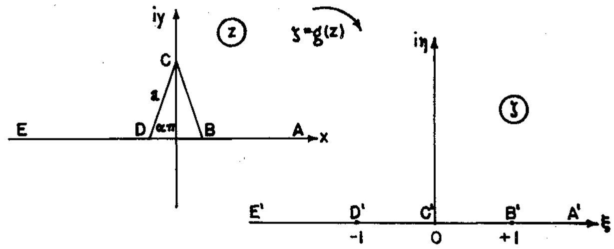

Fig. 3 Physical and mapped half-planes, diamond ring-wing.

Miles[4] has given M in terms of the analytic function that maps P onto a circle. For the shapes considered here it is easier to discuss the conformal mapping that carries P onto a slit along the real axis of the ζ-plane, leaving the distant plane unchanged (Fig. 2). This is just

$$\zeta = g(z) = z + \sum_{n=1}^{\infty} A_n z^{-n} \tag{6}$$

Thus $A_1 = \operatorname{Res} g$. Observe that the inverse mapping is

$$z = g^{-1}(\zeta) = \zeta - A_1\zeta^{-1} + \sum_{n=2}^{\infty} B_n \zeta^{-n} \tag{7}$$

with the derivative

$$\frac{dz}{d\zeta} = 1 + A_1\zeta^{-2} - \sum_{n=2}^{\infty} nB_n \zeta^{-(n+1)} \tag{8}$$

so if only $dz/d\zeta$ is known, the coefficient A_1 can still be picked out of the series expansion.

Diamond Ring-Wing

Invoking symmetry, we restrict attention to the upper half-plane and seek the Schwarz-Christoffel transformation[5] that carries the degenerate polygon ABCDE onto the real axis $\operatorname{Im}\{\zeta\} = 0$ (Fig. 3). Besides leaving infinity unchanged, we can choose the location of C' at $\zeta = 0$ and B at $\zeta = 1$; then by symmetry D' is at $\zeta = -1$. The desired mapping is given by

$$dz/d\zeta = (\zeta + 1)^{-\alpha}\zeta^{2\alpha}(\zeta - 1)^{-\alpha} = \zeta^{2\alpha}(\zeta^2 - 1)^{-\alpha}$$

This has the series expansion in the form (8)

$$dz/d\zeta = (1 - \zeta^{-2})^{-\alpha} \sim 1 + \alpha\zeta^{-2} + 0(\zeta^{-4})$$

so $A_1 = \alpha$ and $M = 2\pi\rho\alpha$. The dimension a is still unknown and must be determined as the definite integral:

$$a(\alpha) = \int_0^1 \xi^{2\alpha}(1 - \xi^2)^{-\alpha} d\xi = \pi^{-1/2}\Gamma(1 - \alpha)\Gamma(\tfrac{1}{2} + \alpha)$$

The dimensionless added mass $M/\rho \cdot \pi a^2$ is exhibited in Table 1 and Fig. 4, as a function of the angle $\beta = (\pi/2) - \alpha\pi$.

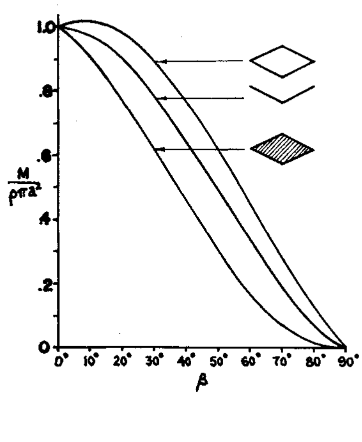

Fig. 4 Dimensionless added mass of three shapes vs dihedral angle.

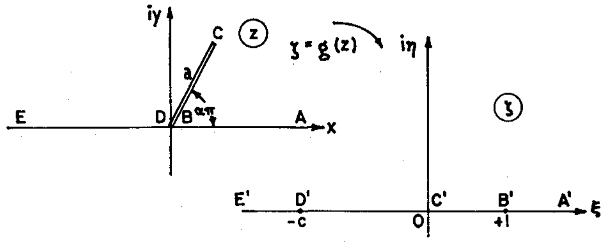

Fig. 5 Physical and mapped half-planes, V-wing.

Table 1. Dimensionless added mass of three shapes vs dihedral angle.

β deg.	$M/\rho\pi a^2$		
0	1.000	1.000	1.000
5	1.015	.992	.960
10	1.017	.974	.908
15	1.005	.944	.846
20	.981	.903	.777
25	.945	.852	.701
30	.896	.792	.621
35	.838	.725	.539
40	.771	.652	.457
45	.697	.576	.378
50	.617	.497	.303
55	.533	.418	.234
60	.448	.341	.173
65	.363	.267	.119
70	.280	.198	.076
75	.201	.135	.042
80	.127	.080	.018
85	.060	.035	.004
90	0.	0.	0.

In case only the exterior fluid is to be counted (5) gives $M' = \rho(2\pi\alpha - a^2 \sin 2\alpha\pi)$. This is also given in Table 1 and Fig. 4.

V-Wing

In the case of straight half-wings with dihedral angle β the proper mapping is (Fig. 5)

$$dz/d\zeta = (\zeta + c)^{-\alpha}\zeta(\zeta - 1)^{-(1-\alpha)}$$

We have again chosen C' at $\zeta = 0$ and B' at $\zeta = 1$, and left a unknown; but now the location of D' is also unknown. For large ζ we have

$$\begin{aligned} dz/d\zeta &= (1 - \zeta^{-1})^{-(1-\alpha)}(1\,c + \zeta^{-1})^{-\alpha} \\ &\sim 1 + [(1 - \alpha) - \alpha c]\zeta^{-1} \\ &\quad + \tfrac{1}{2}[(2 - \alpha)(1 - \alpha) - 2c\alpha(1 - \alpha) + c^2\alpha(1 + \alpha)]\zeta^{-2} + \\ &\quad O(\zeta^{-3}) \end{aligned}$$

Now it is clear that the coefficient of ζ^{-1} must vanish to avoid a $\log \zeta$ term in the mapping (7): thus $c = (1 - \alpha)/\alpha$. The coefficient of ζ^{-2} then reduces to $A_1 = (1 - \alpha)/2\alpha$, so $M = \pi\rho(1 - \alpha)/\alpha$. As before, a is found as the definite integral

$$a(\alpha) = \int_0^1 (1 - \xi)^{-(1-\alpha)}(c + \xi)^{-\alpha}\xi \, d\xi$$

In this case the integral could not be reduced to a tabulated form, so it was evaluated numerically. The dimensionless added mass $M/\rho \cdot \pi a^2$ is given in Table 1 and Figure 4 as a function of the angle $\beta = (\pi/2) - \alpha\pi$.

References

[1] Cone, C. D., "The Theory of Induced Lift and Minimum Induced Drag of Non-planar Lifting Systems," TR-139, 1962, NASA.

[2] Munk, M. M., "The Minimum Induced Drag of Aerofoils," Report 121, 1921, NACA.

[3] Lamb, H., *Hydrodynamics*, 6th ed., Dover, New York, 1932, p. 90.

[4] Miles, J. W., "Virtual Momentum and Slender Body Theory," *Quarterly Journal of Mechanics and Applied Mathematics*, Vol, 6, Part 3, 1953, pp. 286–289.

[5] Carrier, G. F., Krook, M. and Pearson, C. E., *Functions of a Complex Variable*, McGraw-Hill, New York, 1966, p. 142.

Lift on Airfoils with Separated Boundary Layers

NATHAN NESS*
West Virginia University, Morgantown, W. Va.

THIS Note contains the salient features of a method for calculating the sectional lift coefficient c_l on an airfoil as a function of its angle of attack α and freestream Reynolds number Re_∞ ($= V_\infty c/\nu_\infty$) even at large angles of attack beyond the maximum c_l. The details of the method are contained in Ref. 1 which also contains the computer program.

The theory proceeds as follows. An angle-of-attack α, a lift coefficient c_l, and a freestream velocity V_∞ are assumed and the Theodorsen method[2] is used to locate the forward stagnation point and the inviscid flow over the body. A boundary-layer analysis starting at the forward stagnation point and proceeding downstream along the upper and lower surface is then performed. The initial flow is laminar and then may become turbulent. The boundary layer is analyzed by using the Cebeci, Smith[3] finite-difference method in both the laminar and the turbulent regions. In the turbulent region, the boundary-layer equations are expressed in terms of an eddy-viscosity coefficient while in the laminar region the eddy-viscosity coefficient is set equal to zero. Transition from laminar to turbulent flow is based on a momentum Reynolds number of 640 for a favorable pressure gradient and of 320 for an unfavorable pressure gradient. Included in the transition criteria (should they be needed) are experimental relations proposed by Gaster[4] for the bursting of short laminar separation bubbles.

The boundary-layer calculations are carried downstream until separation, characterized by a zero shear stress at the surface, results. At the point of zero shear stress (the separation point) the pressure coefficient c_p is known from the Theodorsen inviscid analysis. The pressure coefficients at separation on the upper and lower surfaces are then plotted against the assumed c_l (Fig. 1).

The calculations (inviscid plus boundary layer) are repeated for other assumed c_l keeping α and Re_∞ constant, until the

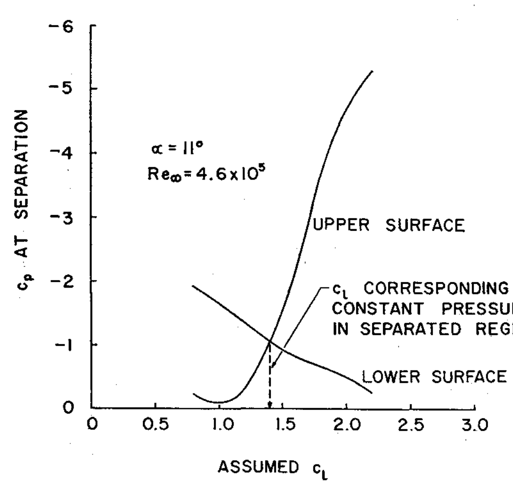

Fig. 1 Determination of c_l for prescribed values of α and Re_∞.

Received April 10, 1972. This work was developed for the Office of Naval Research under Navy V/STOL Aerodynamics Contract N00014-68-A-0512. The author acknowledges E. H. Gibbs, Instructor, and W.-A. P. Tseng, Graduate Research Assistant, both Department of Aerospace Engineering, West Virginia University, for programing and performing the present calculations.

Index category: Airplane and Component Aerodynamics.

* Professor of Aerospace Engineering. Associate Fellow AIAA.